The Fluorescence and Infrared Absorption Probe para-Cyanophenylalanine: Effect of Labeling on the Behavior of Different Membrane-Interacting Peptides

Journal:	*Biopolymers: Peptide Science*
Manuscript ID:	BIP-PEP-2015-00021.R1
Wiley - Manuscript type:	Original Article
Date Submitted by the Author:	n/a
Complete List of Authors:	Bobone, Sara; University of Rome Tor Vergata, Department of Chemical Sciences and Technologies De Zotti, Marta; Institute of Biomolecular Chemistry, CNR, Padova Unit, University of Padova, Department of Chemistry Bortolotti, Annalisa; University of Rome Tor Vergata, Department of Chemical Sciences and Technologies Biondi, Barbara; Institute of Biomolecular Chemistry, CNR, Padova Unit, University of Padova, Department of Chemistry Ballano, Gema; University of Padova, Chemistry Palleschi, Antonio; University of Rome Tor Vergata, Department of Chemical Sciences and Technologies Toniolo, Claudio; University of Padova, Chemistry Formaggio, Fernando; University of Padova, Chemistry Stella, Lorenzo; University of Rome Tor Vergata, Department of Chemical Sciences and Technologies
Keywords:	alamethicin, para-cyano aromatic probe, fluorescence, infrared absorption, peptide synthesis

The Fluorescence and Infrared Absorption Probe *para*-Cyanophenylalanine: Effect of Labeling on the Behavior of Different Membrane-Interacting Peptides

Sara Bobone,[1,#,§] Marta De Zotti,[2,#] Annalisa Bortolotti,[1] Barbara Biondi,[3] Gema Ballano,[2] Antonio Palleschi,[1] Claudio Toniolo,[2,3] Fernando Formaggio,[2,3,*] Lorenzo Stella[1,*]

submitted for the Special Issue of Biopolymers (Pept. Sci.) devoted to the contributions presented at the "Peptides in Paris Symposium-PIPS 2014"

[1] Department of Chemical Sciences and Technologies, University of Rome "Tor Vergata", 00133 Rome, Italy

[2] Department of Chemistry, University of Padova, 35131 Padova, Italy

[3] Institute of Biomolecular Chemistry, Padova Unit, CNR, 35131 Padova, Italy

---

[#] These authors contributed equally

[§] Current address: Institute für Biologie, Humboldt – Universität zu Berlin, 10115 Berlin, Germany

[*] *Correspondence to*: Lorenzo Stella; e-mail: stella@stc.uniroma2.it and Fernando Formaggio; e-mail: fernando.formaggio@unipd.it

ABSTRACT

Total syntheses and complete characterizations of singly substituted Phe_{CN}-based analogs of alamethicin **AlaP**, which is active on model and natural membranes, and the **TM** peptide, which inserts in a trans-membrane orientation in lipid bilayers, are reported. The syntheses of the **AlaP** analogs were performed in solution, while those of **TM** and its analogs were carried out by solid phase. Using the cyanophenyl fluorescence and IR absorption probe, an in-depth investigation of the self-association, membrane-interacting, permeabilizing, and orientation properties of these peptides were conducted. The aromatic residue incorporated induces only a negligible modification to the properties of the parent peptides. The Phe_{CN} IR absorption band was located between 2228-2230 cm^{-1} for all peptides, irrespective of the position of labeling. By contrast, as the width of this band varied significantly with the depth of probe insertion in the bilayer, it could represent a good marker of the Phe_{CN} position in phospholipid membranes.

Keywords: alamethicin, *para*-cyano aromatic probe; fluorescence; infrared absorption; peptide synthesis.

INTRODUCTION

Phe_{CN} is an α-amino acid with interesting IR absorption and emission (in the UV region) properties.[1-27] Its IR absorption band is centered at approximately 2230-2240 cm^{-1}, *i.e.* in a spectral region completely free of overlap with other bands. In addition, the position of this band is sensitive to the environment. In particular, it is dependent on the local electric field, and thus on polarity. The maximum shifts from 2237.2 cm^{-1} (FWHM 9.8 cm^{-1}) in water to 2228.5 cm^{-1} (FWHM 5.0 cm^{-1}) in tetrahydrofuran. For this reason, it has been used as an environmental probe in studies of protein and peptide conformations and interactions. In particular, a few investigations reported the IR absorption properties of the Phe_{CN} probe for peptides associated to bicelles[15] or phospholipid membranes.[3,25,27] However, a simplistic analysis of the band properties in terms of local electric field is not warranted, because of the additional dependence of the IR absorption peak on H-bond formation, solvent dynamics and other more complex electrostatic interactions.[28,29] Also the fluorescence properties of Phe_{CN} are useful. In water, its quantum yield is 0.11, compared to 0.025 for the extremely weak Phe emission. In addition, this parameter is strongly sensitive to the environment, H-bond formation, and the presence of Cl^- and other ions. For instance, the quantum yield and lifetime of Phe_{CN} decrease dramatically in apolar environments. These properties can be exploited to follow peptide aggregation or water-membrane partition, but, at the same time, they might somehow hamper the application of the fluorescence of this probe in the characterization of peptides inserted inside membranes. Finally, compared to other fluorescent or IR extrinsic probes, Phe_{CN} is rather noninvasive, as it is an amino acid which sterically is very similar to Tyr.

The present study is aimed at defining the usefulness of Phe_{CN} in studies of membrane-interacting peptides. One of the most important properties of a spectroscopic probe is a minimal perturbation of the behavior of the system where it is introduced. This characteristic is vital for peptides, since probe-induced perturbations might be particularly relevant for these relatively small biomolecules. To test this aspect for Phe_{CN}, we concentrated on labeled analogs of two membrane-interacting peptides that had previously been extensively characterized: (i) the peptaibiotic[30,31] alamethicin,[32-54] rich in the strongly helicogenic Aib residues,[55-60] the second compound of this class, after trichogin,[61-63] to be labeled with a *para*-cyano aromatic probe,[26,27] and (ii) a model helical peptide (**TM**),[64] which has been demonstrated to reliably insert in a trans-membrane orientation. The sequences and acronyms of the compounds investigated are reported in Table I. The alamethicin analog **AlaP**, which we showed in a previous study to behave similarly to the naturally-occurring peptaibiotic,[36,37] was labeled at three different positions (4, 9, and 15, *i.e.* near the N-terminus, in a central position, and near the C-terminus, respectively) along its main chain. For the **TM** peptide analogs, the probe was inserted at position 3 (peptide **TM3**) or 11 (peptide **TM11**), which should be positioned in a very different membrane environment when the peptides insert in a transmembrane orientation. In particular, considering the known helical conformation of **TM**,[64] the probe would be located at approximately 15 and 3 Å from the center of the bilayer for **TM3** and **TM11**,

respectively. These variants will allow an assessment of the sensitivity of the spectroscopic properties of the probe to the depth of its immersion in the membrane. In all analogs Phe_{CN} replaces an apolar residue (Ala, Val or Leu). A preliminary report of a limited part of this work was already presented.[26]

MATERIALS AND METHODS

Abbreviations and Materials

Ac, acetyl; Aib, α-aminoisobutyric acid; ATR, attenuated total reflectance; Boc, *tert*-butyloxycarbonyl; CD, circular dichroism; CF, carboxyfluorescein; DCM, dichloromethane; DIEA, diisopropylethylamine; DMF, N,N-dimethylformamide; EDC, N-ethyl, N'-[3-(dimethylamino)propyl]carbodiimide; ESI-MS, electrospray ionization-mass spectrometry; Fmoc, 9-fluorenylmethyloxycarbonyl; FT, Fourier transform; FWHM, full width at half maximum; HATU, O-(7-azabenzotriazol-1-yl)-1,1,3,3-tetramethyluronium hexafluorophosphate; HBTU, O-(benzotriazol-1-yl)-1,1,3,3-tetramethyluronium hexafluorophosphate; HOAt, 7-aza-1-hydroxy-benzotriazole; HOBt, 1-hydroxy-benzotriazole; IR, infrared; LL, low loading; MBHA, 4-methyl-benzhydrylamine; MS, mass spectrometry; MW, molecular weight; NMM, N-mehylmorpholine; OAll, allyloxy; OBzl, benzyloxy; OMe, methoxy; Phe_{CN}, *para*-cyanophenylalanine; PEG, polyethylene glycol; Phol, phenylalaninol; POPC, 1-palmitoyl-2-oleoyl-*sn*-glycero-3-phosphocholine; RP-HPLC, reverse-phase high performance liquid chromatography; SDS, sodium dodecyl sulphate; SPPS, solid-phase peptide synthesis; TIS, triisopropylsilane; TFA, trifluoroacetic acid.

All amino acids and derivatives used, including Fmoc-Lys(Boc)-OH, were of L- configuration and purchased from IRIS Biotech (Marktredwitz, Germany) or Sigma-Aldrich (St. Louis, MO). EDC, HOBt, HOAt, HATU, and HBTU were GL Biochem (Shanghai, China) products. SDS was obtained from Acros (Geel, Belgium). POPC was purchased from Avanti Lipids (Alabaster, AL). All other chemicals were obtained from Sigma-Aldrich (St. Louis, MO). Spectroscopic grade solvents were used in all CD and fluorescence experiments. ESI-MS data were recorded on a PerSeptive Biosystem Mariner Instrument (Farmingham, MA).

Peptide Synthesis in Solution

The three Phe_{CN}-containing **AlaP** analogs were synthesized by solution-phase methodologies using a combination of step-by-step and segment condensation approaches. As an example, the strategy followed for the synthesis of **AlaP** is reported in **Scheme 1**. All synthetic intermediates were fully characterized by physical and analytical techniques (*Supporting Information*).

Solid-Phase Peptide Synthesis

Assembly by automatic SPPS of the three **TM** peptides on the Advanced ChemTech (Louisville, KY) 348 Ω peptide synthesizer was performed on a 0.03 mmol scale by the FastMoc methodology [HBTU,[65] HOBt,[66] DIEA, double acylation protocol, 45 min coupling time, N-methylpyrrolidin-2-one as the solvent], using the Rink Amide MBHA LL resin (Novabiochem, Darmstadt, Germany) (100 mg, loading 0.30 mmol g^{-1}). Removal of the Fmoc group was performed with a 20% piperidine solution in DMF in two steps of 5 and 15 min, respectively. The chromatographically purified, final peptides were fully characterized (*Supporting Information*).

UV-Vis Absorption

UV-vis absorption measurements were carried out on a Cary 100 Scan (Varian, Palo Alto, CA) spectrophotometer. Molar concentrations of the labeled analogs were determined in MeOH solution at λ=280 nm [Phe_{CN} absorption, ε(280 nm)=850 M^{-1} cm^{-1}].[5]

Circular Dichroism

CD measurements were carried out on a *Jasco J-715* spectropolarimeter. The CD spectra were acquired and processed using the *J-700* program for *Windows*. All spectra were recorded at room temperature, using *Hellma* quartz cells with *Suprasil*® windows and optical path lengths of 0.1 cm. The signal-to-noise ratio was improved by accumulating eight scans. The values are expressed in terms of total molar ellipticity, $[\theta]_T$ [deg·cm^2·$dmol^{-1}$]. MeOH and 100 mM aqueous SDS were used as solvents.

Steady-State Fluorescence

Fluorescence experiments were performed on a Fluoromax-4 fluorimeter (Horiba-Jobin Yvon, France), under the following conditions: λ_{exc}=240 nm, bandpass: 10 nm in excitation, 2 nm in emission; integration time=2 s, peptide concentration = 1μM; T=25 °C.

Time-Resolved Fluorescence

Fluorescence intensity decays were measured on an Edinburgh Instruments [Edinburgh, UK], time-correlated single photon counting setup, using a nanosecond flash-lamp filled with nitrogen for excitation. Experimental conditions: λ_{exc}= 240 nm; λ_{em} = 295 nm, interval: 50 ns, channels: 1024, bandwidth: 10 nm.

Liposome Preparation

Large unilamellar vesicles were prepared as previously described,[67] by dissolving POPC lipids in a 1:1 (vol/vol) methanol/chloroform solution, in an appropriate amount to obtain a final stock solution of liposomes with a lipid concentration of 5 mM. The solvents were evaporated under reduced argon

atmosphere until a thin film was formed. Complete evaporation was ensured by applying a rotary vacuum pump for at least 2 hr. The lipid film was hydrated with a 10 mM phosphate buffer (pH 7.4), 140 mM NaCl and 0.1 mM EDTA (buffer A, used for water-membrane partition experiments) or with a CF solution prepared by dissolving the dye powder in a minimum amount of 0.1 M NaOH, and then diluting to 30 mM CF in 10 mM phosphate buffer (pH 7.4), 80 mM NaCl and 0.1 mM EDTA (for membrane perturbation experiments).[68] The iso-osmolarity of these solutions was checked with a freezing point depression osmometer (Fiske-Advanced Instruments, Norwood, USA). After vigorous stirring and 10 freeze and thaw cycles, the liposome suspension was extruded for 31 times through two stacked polycarbonate membranes (Avestin, Ottawa, ON, Canada) with pores of 100 nm or 200 nm diameter (see below). The unencapsulated fluorescent tracer was separated from the liposomes by gel filtration on a Sephadex G-50 medium column (40cm) in buffer A. Lipid concentration in the final sample was determined by the Stewart method.[69]

Water-Membrane Partition

Water-membrane partition experiments were performed by titrating a 1 µM peptide solution (in buffer A) with increasing amounts of a lipid vesicles solution, and by following the variation in the emission intensity . The cuvette was pretreated for 30 min with a 5% (w/w) solution of PEG, to avoid peptide adsorption to the quartz walls. The fraction of peptide associated with membranes was calculated from the fluorescence intensity at 292 nm (*F*), according to the following equation:

$$f = \frac{F - F_M}{F_M - F_W},$$

where F_W and F_M represent the fluorescence intensities of the peptide in water and in the membrane, respectively. The value of F_M was extrapolated by a double reciprocal plot of 1/*F vs* 1/[*POPC*]. The partition curve was fit with the following equation:[70,71]

$$f = \frac{K_P \frac{[POPC]}{55.3\ M}}{1 + K_P \frac{[POPC]}{55.3\ M}}$$

where 55.3 M is the molarity of pure water at 25 °C, and $K_P = \frac{x_p^L}{x_p^W}$ is the partition constant defined as the ratio of molar fractions of the peptide in the lipid and water phases at equilibrium.[67,70] Since the partition data were essentially superimposable for the different alamethicin analogs, they were fit globally with a single curve, yielding K_P=4.0 10^3. Experimental conditions: [POPC]= from 0.1 to 50 µM; λ_{exc}= 240 nm; band-pass 3 nm in excitation and 5 nm in emission; liposome diameter: 100 nm; T=25°C. The background due to liposome scattering was subtracted from each spectrum.

Membrane-Perturbing Activity

CF-loaded liposomes (with 200-nm diameter) were used to assess the membrane-perturbing activity of the compounds. The peptide-induced leakage from vesicles was measured 20 min after peptide addition. The leaked fraction was calculated as

$$R = \frac{F - F_0}{F_{100} - F_0}$$

where F_0 is the CF signal before peptide addition, and F_{100} is the intensity after the addition of a detergent, triton-X100 1 mM, which causes complete lysis of membranes. F is the fluorescence value obtained 20 min after peptide addition.[72, 73] Experimental conditions: λ_{exc}= 490 nm (bandwidth 0.2 nm); λ_{em}= 520 nm (bandwidth 1.5 nm); [POPC]: 20 μM; T=25°C.

Fluorescence Quenching

Fluorescence quenching data were analyzed according to a model with two sub-populations of the peptide, contributing to the overall fluorescence with fractions f_1 and $f_2=1- f_1$, and different accessibilities to the quencher, resulting in different values for the Stern-Volmer constants, K_1 and K_2:[74]

$$\frac{F_0}{F} = \left\{ \frac{f_1}{1 + K_1[Q]} + \frac{1 - f_1}{1 + K_2[Q]} \right\}^{-1}$$

The following values were derived for the experiments performed with the **TM** analogs:

TM3: f_1=0.42±0.01, K_1=3.3±0.9 mM^{-1}, K_2=(1.9±0.6) 10^{-3} mM^{-1}.

TM11: f_1=0.36±0.01, K_1=0.46±0.05 mM^{-1}, K_2=0 mM^{-1}.

ATR-FTIR Absorption

Infrared absorption measurements were performed on a Nicolet FTIR spectrometer (Thermo Electron Co., Madison, WI) in the ATR mode. A 1:1 chloroform/methanol solution of POPC and peptide (1.5 μmoles of POPC with 5%, or 15% molar fraction of peptide, for **TM** and **AlaP** analogs, respectively) was spread onto a 8x1x0.3 cm Ge crystal (reflection angle 45°, 12 reflections on the sample surface). The total solution volume was 130 μl. The crystal was dried under a gentle Ar stream and then put under vacuum for 2 hr to completely remove the organic solvents. The sample was hydrated by placing a water-containing vessel into a gas-tight chamber onto the Ge crystal. Spectra were acquired every hour for 8-12 hr. After the first 2 hr, no modifications in the position or intensities of the bands were revealed during the experiment, indicating the attainment of equilibrium in hydration. ATR spectra were acquired under the following conditions: 2 cm^{-1} resolution, 128 acquisitions (256 for the polarized spectra). The FWHM of the cyano peak was determined by fitting the absorption band to a Gaussian function.

For polarized ATR experiments, the ATR electric fields of the incident light were calculated considering a refractive index of 4 for Ge and of 1.44 for the lipids.[75] Calculations of peptide orientation were carried out

in the thick film approximation, considering that the dichroic ratio of symmetric lipid CH_2 stretching bands is always higher than 1.41.[75] This finding is consistent with the amount of lipids spread on the film, which, considering an area per lipid of 0.68 nm^2,[76] is sufficient to form more than 350 bilayers on the crystal surface. With a bilayer spacing of 6.4 nm at full hydration,[76] it corresponds to a thickness of more than 2 μm, to be compared with a calculated penetration depth (*dp*).[75] This parameter can be obtained according to the following equation:[75]

$$dp = \frac{\lambda}{2\pi\sqrt{(n_1 sin\vartheta)^2 - (n_2)^2}}$$

where λ is the wavelength (6 μm for the amide I band), n_1 and n_2 are the refractive indexes of Ge (4.0) and lipids (1.44), respectively, and ϑ is the reflection angle of the crystal (45°). Therefore, in our case *dp*=0.4 μm and a sample thicker than 2 μm fully justifies the thick film approximation.[75]

The order parameter S was derived from the following equation:[37,75]

$$R = \frac{E_X^2}{E_Y^2} + \frac{E_Z^2}{E_Y^2}(1 + \frac{3S}{1-S})$$

$R = {}^{A_\parallel}/_{A_\perp}$ is the dichroic ratio of the peptide amide I band calculated by integrating the absorbance measured between 1600 and 1700 cm^{-1} with light polarized parallel $(A_\parallel)$ and perpendicular $(A_\perp)$ to the incidence plane. The three components of the electric fields are given by E_x= 1.40, E_y=1.52, E_z=1.62,[75] and *S* corresponds to

$$S = \frac{3 < cos^2\alpha > -1}{2} \quad \frac{3 < cos^2\beta > -1}{2}$$

where α is the angle between the helix axis and the membrane normal, and β is the angle between the transition dipole of the IR absorption band and the helix axis. In the case of helical peptides, the value of β can be taken equal to 38°.[75]

RESULTS AND DISCUSSION

Synthesis of the AlaP Analogs in Solution

The syntheses of the **AlaP** analogs are complicated by the presence of two Aib-Pro tertiary amide bonds in the sequences and the limited reactivity of the eight sterically hindered, C^α-tetrasubstituted Aib residues, particularly at their N-side.[36, 77-80] However, luckily under the coupling conditions used the –OH function of the C-terminal Phol 1,2-aminoalcohol is known to be extremely poorly reactive.[36]

In the present work, we applied our published synthetic strategy for the solution synthesis of **AlaP** analogs,[36] slightly modifying it to insert the residue containing the *para*-cyanoaromatic probe. Briefly, the

sequence was divided into three segments (**A**, **B**, and **C**) (Schemes 1 and 2) at the level of the Aib-Ala and Aib-Pro bonds. The segments were synthesized step-by-step and eventually condensed to afford the final **AlaP** analogs. The protecting groups were chosen to minimize the reaction time and to avoid the use of strong reductive conditions in the presence of the sensitive cyano group. The activating agents for the coupling reactions (EDC/HOAt)[81] were selected by taking into account the low reactivity of the Aib residue. The sequences of the three analogs were split as reported in Scheme 2. The reaction yields of the several synthetic steps were from moderate to good. Eventually, we obtained our target **AlaP** analogs in good amounts (about 100 mg each) and purity (> 96%).

Solid-Phase Synthesis of the TM Analogs

In the two analogs of the 24-mer **TM** peptide the Phe_{CN} residue was introduced near the N-terminus (position 3) and in the central region (position 11), respectively, in both cases replacing a similarly hydrophobic Leu residue (Table I).The three syntheses were performed in parallel. The Rink Amide MBHA LL resin and our protocol were chosen to better avoid peptide aggregation. As for the latter: (1) Fmoc deprotection of the N^{α}-function was achieved with a 20 % piperidine solution in DMF in two steps of 5 and 15 min each. The reaction times were extended to 10 and 25 min, respectively, for the two Lys residues at positions 1 and 2 in the sequence. (2) Coupling reactions (each repeated twice) were carried out using the standard activation method *via* HBTU/HOBt.[65,66] (3) N-Terminal acetylation of the final N^{α}-deprotected peptides was performed by two treatments with acetic anhydride and DIEA in DMF for 30 min each. (4) Cleavage of the peptides from the resin was obtained using a TFA/H_2O/TIS mixture (95:5:5 *v*/*v*, 5 ml/100 mg of peptide resin, 2 hr at room temperature). The solution was concentrated and the peptide precipitated by addition of diethyl ether. The desired final peptides were isolated in 75–80 % average yield. Subsequently, the crude peptides were purified by *semi*-preparative HPLC using a Vydac column and characterized by analytical RP-HPLC and ESI-MS (*Supporting Information*).

Spectroscopic Properties of the Phe_{CN}-Labeled Peptides

All analogs exhibit the typical fluorescence and IR absorption spectra of the Phe_{CN} probe

Figure 1 shows the normalized fluorescence spectra of the **AlaP** analogs at a 1 μM concentration in an aqueous buffer composed of 10 mM phosphate buffer, 140 mM NaCl, and 0.1 mM EDTA (pH 7.4). The same buffer was used in all of the following experiments. Spectra show the typical shape of Phe_{CN} emission, with a maximum at 293 nm. No differences among the analogs were found. Similar spectra were obtained for all three **TM** peptides (data not shown). The IR absorption band of the C≡N probe for **Ala9** in MeOH exhibits wavelength maximum and FWHM value comparable to those of the isolated amino acid (2231±12 and 2232±11 cm^{-1}, respectively).

Effects of the Phe_{CN} Probe on Peptide Behavior

Phe_{CN} does not perturb the peptide secondary structure

The secondary structure of all peptides in MeOH and in the membrane-mimicking SDS environment was characterized by use of far-UV CD (Figure 2). All spectra indicate a predominantly right-handed helical conformation,[82-85] which is similar to those of the parent peptides, suggesting that the probe does not significantly affect peptide conformation. The remarkably different ellipticity ratios (*R* values) at 222 nm *versus* 208 nm[84,85] for all peptides, higher in SDS micelles (particularly for the **AlaP** analogs), point to a significant increase of the α-helix percentage at the expenses of the 3_{10}-helix under the latter condition. The contributions of the aromatic toluene-based Phol and Phe_{CN} chromophores to the CD curves in this spectral region[82,83] do not seem to complicate the interpretation of the spectroscopic results.

*Phe_{CN} does not perturb the aggregation of the **AlaP** peptides in water*

The parent, unlabeled peptide **AlaP** was previously demonstrated to aggregate in water.[37] To test whether the introduction of the Phe_{CN} probe in place of an Ala or Val residue would significantly perturb peptide aggregation in water, we exploited the fluorescence properties of the probe to assess the self-association behavior of the three analogs. Fluorescence intensity decays were measured at increasing peptide concentrations in the presence of quenching Cl^- ions[86] (140 mM NaCl). Since these anions quench the fluorescence of Phe_{CN} collisionally, we expected a significantly different fluorescence lifetime for monomers and aggregates (where the fluorophores are partially shielded from the solvent). Indeed, the Phe_{CN} decays of each alamethicin analog at different concentrations (Figure 3) could be analyzed globally as the sum of two exponentials, with a global reduced chi square always lower than 1.2. The two components likely correspond to the monomeric peptide (short lifetime, *i.e.* 3.4 ± 0.6 ns, 4.0 ± 0.2 ns and 4.0 ± 0.2 ns for Ala4, Ala9 and Ala15, respectively) and aggregated species (long lifetime, *i.e.* 10.0 ± 0.5 ns, 11.0 ± 0.4 ns, 10.1 ± 0.7 ns for Ala4, Ala9 and Ala15, respectively). Therefore, the pre-exponential factor of the long lifetime provides a measure of the population of the aggregated species (Figure 4). The behavior of the three analogs is quite similar. In particular, they exhibit a strong tendency to aggregate. Monomers are practically absent already at a concentration of 10 μM (Figure 4). This aggregation behavior is strongly reminiscent of that previously determined for the parent peptide **AlaP** by CD measurements,[37] indicating that no significant perturbation is introduced by the Phe_{CN} fluorophore, except for a slightly higher tendency to aggregate for the Ala to Phe_{CN} substituted analog.

*Phe_{CN} does not perturb the peptide affinity of the **AlaP** peptides for membranes*

Peptide-membrane interaction is a fundamental step in the activity of membrane-active peptides. Therefore, we checked whether Phe_{CN} introduction would perturb the affinity of the **AlaP** analogs for lipid bilayers, the membrane-binding affinity of which was determined previously.[37] Experimentally, peptide

association to membranes was followed by variation in the fluorescence intensity of the Phe_{CN} probe. The emission spectra of **Ala15** in the absence and presence of increasing amounts of lipid vesicles are reported in Figure 5. Similar spectra were obtained for **Ala4** and **Ala9** (data not shown). The intensity in water is higher than that in the membrane, probably due to H-bond formation by the cyano group in water.[12] The partition curve resulted to be essentially the same for all of the analogs (Figure 6), notwithstanding the different position of the probe in the sequence. This finding once more indicates that perturbations introduced by Phe_{CN} are negligible.

*Phe_{CN} does not perturb the membrane permeabilizing activity of the **AlaP** peptides*

A more stringent, overall test of peptide behavior in the membrane is provided by its membrane permeabilizing activity, which is mediated by both aggregation and lipid binding equilibria.[37] CF-loaded liposomes were used to assess the membrane-perturbing activity of the analogs. The fraction of liposome contents leaked 20 minutes after peptide addition is reported in Figure 7. All peptides exhibit a behavior very close to that of the parent peptide **AlaP**, confirming that the probe does not interfere with peptide activity.

*Phe_{CN} does not perturb the trans-membrane insertion of the **TM** analogs*

The transmembrane orientation of the **TM** analogs labeled with PheCN was studied by fluorescence quenching and polarized ATR-FTIR experiments. Quenching by chloride ions[13,14] of the peptides embedded inside lipid vesicles [50 μM lipids and 3 μM peptide] is reported in Figure 8. The nonlinear behavior of the Stern-Volmer plots indicates a heterogeneity in the probe accessibility, and was fit with a model having two sub-populations of the peptide with different accessibilities of the Phe_{CN} residue to the quencher (see Materials and Methods). In any case, **TM3** is much more sensitive to the Cl^- ions than **TM11**, showing that the Phe_{CN} probe inserted at position 3 is more exposed to the water phase and corroborating our view of its more superficial positioning. Polarized ATR spectra of the amide I absorption band confirmed the transmembrane orientation of the **TM** analogs. The ratio of absorbance values measured with a polarization parallel and perpendicular to the incidence plane (dichroic ratio) indicates a cosine squared of the angle between the peptide helix and the bilayer normal of about 0.7 (see Materials and Methods), which corresponds to an average angle of about 30° (Figure 9).

Sensitivity of the Phe_{CN} IR Absorption Band to the Depth of Peptide Insertion in the Membrane

The experiments reported earlier in the text indicate that the Phe_{CN} fluorescence can be usefully employed to study peptide aggregation, membrane binding, and position in the bilayer. Based on these findings, the **TM** analogs can be considered as a sort of calibration for the sensitivity of the cyano IR absorption band to the depth of the peptide insertion in the membrane. To study the IR absorption properties of the Phe_{CN}

probe in membranes, the ATR-FTIR spectra of the **AlaP** and **TM** analogs were recorded in supported POPC bilayers. As an example, the overall spectrum of **Ala15** (P/L=15%) is illustrated in Figure 10, while the Phe_{CN} band is shown in Figure 11 for both **TM3** and **TM11**. Peak position and width are reported in Table 2 for all analogs. Surprisingly, irrespective of the specific peptide and the labeling position, the band peak is located in a very narrow interval (approximately between 2228 and 2230 cm^{-1}), *i.e.* in a range corresponding to the values observed for aprotic solvents.[29] Also the few previous studies on the IR absorption properties of Phe_{CN}-labeled peptides interacting with membrane-mimicking environments reported similar spectra,[3,15,25,27] even when other evidence pointed towards a significant solvent exposure of the residue.[3,25] Further studies will be needed to understand why this type of probe inserted at varying membrane depths does not sense a different environment, since in a lipid bilayer the local polarity and water penetration change from the bilayer surface down to less than 1.5 nm from the membrane center.[87,88] However, the position of the aromatic C≡N IR absorption band is influenced by several factors, including local electric field and hydrogen bonding,[29] which in the complex environment of the membrane might combine to produce the observed lack of sensitivity to the depth of insertion in the bilayer.

Variations in the width of the absorption band are much more significant, since the FWHM for **TM3** is almost twice that of **TM11**. This finding suggests that the bandwidth decreases with the depth of insertion, and is consistent with experiments in pure solvents, , which reported a width of 10 cm^{-1} in water and 5 cm^{-1} in tetrahydrofuran.[1] In addition, previous investigations on cationic peptides bound to the surface of the membrane[3] and on peptides reminiscent of the **TM** analogs investigated here, but inserted in bicelles rather than in lipid bilayers,[15] reported a similar trend of reduction in IR absorption bandwidth upon membrane insertion.

A large bandwidth was observed for all membrane-associated **AlaP** analogs, which indicates a peptide location relatively close to the membrane surface. The orientation of alamethicin in membranes has been the object of multiple studies, which overall point to a concentration-driven transition from a superficial peptide location to a transmembrane arrangement. However, the exact orientation is strongly dependent on several aspects of the sample, including degree of hydration, lipid composition, temperature, and pH.[34,89-92] In addition, in the absence of a transmembrane potential, the peptide C-terminus is always exposed to the solvent.[37] Therefore, it is possible that, under the experimental conditions employed in this study, the Phe_{CN} probe in the **AlaP** analogs locates close to the bilayer surface. On the other hand, X-ray scattering,[93] polarized ATR-FTIR,[37] NMR,[94] and molecular dynamics simulations[95] data indicate a high degree of mobility and heterogeneity in peptide orientation in the membrane in the absence of a transmembrane potential. Therefore, the broad Phe_{CN} absorption bandwidth observed for the **AlaP** analogs might also result from a significant orientational dynamics of the peptide.

CONCLUSIONS

We synthesized and fully characterized analogs of the two long membrane-interacting peptides **AlaP** e **TM** *via* solution-phase synthesis or SPPS, respectively.

A detailed investigation of the aggregation, membrane-binding and membrane permeabilizing behavior of the **AlaP** analogs, and of the orientation of the **TM** peptides in membranes indicated that Phe_{CN} does not perturb significantly even a relatively small molecule such as an oligopeptide. The fluorescent properties of Phe_{CN} were extremely useful in the characterization of all these aspects. Even if no significant spectral shifts are observed for the maximum of the emission band, its intensity is highly sensitive to polarity.

All of the IR absorption spectra for peptides labeled with the Phe_{CN} probe and associated to lipid bilayers exhibit a band peaked approximately between 2228 and 2230 cm^{-1}, irrespective of the specific probe position along the sequence and peptide orientation inside the membrane. Overall, these data suggest that the position of the Phe_{CN} IR absorption band is not significantly sensitive to the depth of probe insertion in lipid membranes. However, the width of the IR absorption band increased approximately by a factor of 2 on going from a deeply inserted position to a superficial location. The FWHM parameter of the Phe_{CN} IR absorption band could thus represent a diagnostic indicator of positioning of the Phe_{CN} residue inside a phospholipid bilayer.

REFERENCES

1. Getahun, Z.; Huang, C.-Y.; Wang, T.; De Leon, B.; DeGrado, W. F.; Gai, F. J Am Chem Soc 2003, 125, 405-411.

2. Huang, C. Y.; Wang, T.; Gai, F. Chem Phys Lett 2003, 371, 731-738.

3. Tucker, M. J.; Getahun, Z.; Nanda, V.; DeGrado, W. F.; Gai, F. J Am Chem Soc 2004, 126, 5078-5079.

4. Tucker, M. J.; Oyola, R.; Gai, F. J Phys Chem B 2005, 109, 4788-4795.

5. Tucker, M. J.; Oyola, R.; Gai, F. Biopolymers 2006, 83, 571-576.

6. Tucker, M. J.; Tang, J.; Gai, F. J Phys Chem B 2006, 110, 8105-8109.

7. Schultz, K. C.; Supekova, L.; Ryu, Y.; Xie, J.; Perera, R.; Schultz, P. G. J Am Chem Soc 2006, 128, 13984-13985.

8. Tang, J.; Signarvic, R. S.; DeGrado, W. F.; Gai, F. Biochemistry 2007, 46, 13856-13863.

9. Mukherjee, S.; Chowdhury, P.; DeGrado, W. F.; Gai, F. Langmuir 2007, 23, 11174-11179.

10. Lindquist, B. A.; Furse, K. E.; Corcelli, S. A. Phys Chem Chem Phys 2009, 11, 8119-8132.

11. Aschaffenburg, D. J.; Moog, R. S. J Phys Chem B 2009, 113, 12736-12743.

12. Serrano, A. L.; Troxler, T.; Tucker, M. J.; Gai, F. Chem Phys Lett 2010, 487, 303-306.

13. Marek, P.; Mukherjee, S.; Zanni, M. T.; Raleigh, D. P. J Mol Biol 2010, 400, 878-888.

14. Taskent-Sezgin, H.; Marek, P.; Thomas, R.; Goldberg, D.; Chung, J.; Carrico, I.; Raleigh, D. P. Biochemistry 2010, 49, 6290-6295.

15. Hu, W.; Webb, L. J. J Phys Chem Lett 2011, 2, 1925-1930.

16. Xu, L.; Cohen, A. E.; Boxer, S. G. Biochemistry 2011, 50, 8311-8322.

17. Levinson, N. M.; Fried, S. D.; Boxer, S. G. J Phys Chem B 2012, 116, 10470-10476.

18. Kim, H.; Cho, M. Chem Rev 2013, 113, 5817-5847.

19. Bazewicz, C. G.; Liskov, M. T.; Hines, K. J.; Brewer, S. H. J Phys Chem B 2013, 117, 8987-8993.

20. Wissner, R. F.; Batjargal, S.; Fadzen, C. M.; Petersson, E. J. J Am Chem Soc 2013, 135, 6529-6540.

21. Levinson, N. M.; Boxer, S. G. Nat Chem Biol 2014, 10, 127-132.

22. Adhikary, R.; Zimmermann, J.; Dawson, P. E.; Romesberg, F. E. Chem Phys Chem 2014, 15, 849-853.

23. Gonzalez, J. D.; Levonyak, N. S.; Schneider, S. C.; Smith, M. J.; Cremeens, M. E. J Mol Struct 2014, 1056-1057, 7-12.

24. Ma, J. Q.; Pazos, I. M.; Gai, F. Proc Natl Acad Sci USA 2014, 111, 8476-8481.

25. Xhindoli, D.; Morgera, F.; Zinth U.; Rizzo R.; Pacor, S.; Tossi, A. Biochem J 2015, 465, 443-457.

26. Bobone, S.; Bortolotti, A.; De Zotti, M.; Ballano, G.; Formaggio, F.; Toniolo, C.; Stella, L. In Proceedings 33rd EPS, Naydenova, E.; Pajpanova, T., Eds.; European Peptide Society, 2015, in press.

27. De Zotti, M.; Bobone, S.; Bortolotti, A.; Longo, E., Biondi, B.; Peggion, C.; Formaggio, F.; Toniolo, C.; Dalla Bona, A.; Kaptein, B.; Stella, L. Chem Biodivers 2015, 12, 513-526.

28. Maienschein-Cline, M. G.; Londergan, C. H. J Phys Chem A 2007, 111, 10020-10025.

29. Fried, S. D.; Boxer, S. G. Acc Chem Res 2015, 48, 998-1006.

30. Toniolo, C.; Brückner, H. Eds.; Peptaibiotics: Fungal Peptides Containing α-Dialkyl α-Amino Acids; Verlag Helvetica Chimica Acta, Zürich, and Wiley-VCH, Weinheim, 2009.

31. Toniolo, C.; Brückner, H., Eds.; Peptaibiotics II; Chem Biodivers 2013, 10, issue No. 5 (Topical Issue).

32. Nagaraj, R.; Balaram, P., Acc Chem Res 1981, 14, 356-362.

33. Fox, R. O., Jr.; Richards, F. M. Nature (London) 1982, 300, 325-330.

34. Sansom, M. S. P. Eur Biophys J 1993, 22, 105-124.

35. Kredics, L.; Szekeres, A.; Czifra, D.; Vagvölgyi, C.; Leitgeb, B. Chem Biodivers 2013, 10, 744-771.

36. Peggion, C.; Coin, I.; Toniolo, C. Biopolymers (Pept Sci) 2004, 76, 485-493.

37. Stella, L.; Burattini, M.; Mazzuca, C.; Palleschi, A.; Venanzi, M.; Coin, I.; Peggion, C.; Toniolo, C.; Pispisa, B. Chem Biodivers 2007, 4, 1299-1312.

38. Peggion, C.; Jost, M.; Baldini, C.; Formaggio, F.; Toniolo, C. Chem Biodivers 2007, 4, 1183-1199.

39. Peggion, C.; Jost, M.; De Borggraeve, W. M.; Crisma, M.; Formaggio, F.; Toniolo, C. Chem Biodivers 2007, 4, 1256-1268.

40. Crisma, M.; Peggion, C.; Baldini, C.; MacLean, E. J.; Vedovato, N.; Rispoli, G.; Toniolo, C. Angew Chem Int Ed 2007, 46, 2047-2050.

41. Milov, A. D.; Samoilova, R. I.; Tsvetkov, Y. D.; Formaggio, F.; Toniolo, C.; Raap, J. J Am Chem Soc 2007, 129, 9260-9261.

42. Marsh, D.; Jost, M.; Peggion, C.; Toniolo, C. Chem Biodivers 2007, 4, 1269-1274.

43. Milov, A. D.; Samoilova, M. I.; Tsvetkov, Y. D.; Jost, M.; Peggion, C.; Formaggio, F.; Crisma, M.; Toniolo, C.; Handgraaf, J.-W.; Raap, J. Chem Biodivers 2007, 4, 1275-1298.

44. Vedovato, N.; Baldini, C.; Toniolo, C.; Rispoli, G. Chem Biodivers 2007, 4, 1338-1346.

45. Milov, A. D.; Samoilova, R. I.; Tsvetkov, Y. D.; De Zotti, M.; Toniolo, C.; Raap, J. J Phys Chem B 2008, 112, 13469-13472.

46. Bartucci, R.; Guzzi, R.; De Zotti, M.; Toniolo, C.; Sportelli, L.; Marsh, D. Biophys J 2008, 94, 2698-2705.

47. Salnikov, E. S.; De Zotti, M.; Formaggio, F.; Li, X.; Toniolo, C.; O'Neil, J. D. J.; Raap, J.; Dzuba, S. A.; Bechinger, B. J Phys Chem B 2009, 113, 3034-3042.

48. Milov, A. D.; Samoilova, R. I.; Tsvetkov, Y. D.; De Zotti, M.; Formaggio, F.; Toniolo, C.; Handgraaf, J.-W.; Raap, J. Biophys J 2009, 96, 3197-3209.

49. Rippa, S.; Eid, M.; Formaggio, F.; Toniolo, C.; Béven, L. ChemBioChem 2010, 11, 2042-2049.

50. Jose, R. A.; De Zotti, M.; Peggion, C.; Formaggio, F.; Toniolo, C.; De Borggraeve, W. M. J Pept Sci 2011, 17, 377-382.

51. Bobone, S.; Roversi, D.; Giordano, L.; De Zotti, M.; Formaggio, F.; Toniolo, C.; Park, Y.; Stella, L. Biochemistry 2012, 51, 10124-10126.

52. De Zotti, M.; Ballano, G.; Jost, M.; Salnikov, E. S.; Bechinger, B.; Oancea, S.; Crisma, M.; Toniolo, C.; Formaggio, F. Chem Biodivers 2014, 11, 1163-1191.

53. Bortolus, M.; Dalzini, A.; Toniolo, C.; Hahm, K.-S.; Maniero, A. L. J Pept Sci 2014, 20, 517-525.

54. Milov, A. D.; Samoilova, R. I.; Tsvetkov, Y. D.; Peggion, C.; Formaggio, F.; Toniolo, C. J Phys Chem B 2014, 118, 7085-7090.

55. Yasui, S. C.; Keiderling, T. A.; Bonora, G. M.; Toniolo, C. Biopolymers 1986, 25, 79-89.

56. Valle, G.; Crisma, M.; Toniolo, C.; Beisswenger, R.; Rieker, A.; Jung, G. J Am Chem Soc 1989, 111, 6828-6833.

57. Karle, I. L.; Balaram, P. Biochemistry 1990, 29, 6747-6756.

58. Toniolo, C.; Benedetti, E. Trends Biochem Sci 1991, 16, 350-353.

59. Bolin, K. A.; Millhauser, G. L. Acc Chem Res 1999, 32, 1027-1033.

60. Toniolo, C.; Crisma, M.; Formaggio, F.; Peggion, C. Biopolymers (Pept Sci) 2001, 60, 396-419.

61. Toniolo, C.; Crisma, M.; Formaggio, F.; Peggion, C.; Monaco, V.; Goulard, C.; Rebuffat, S.; Bodo, B. J Am Chem Soc 1996, 118, 4952-4958.

62. Peggion, C.; Formaggio, F.; Crisma, M.; Epand, R. F.; Epand, R. M.; Toniolo, C. J Pept Sci 2003, 9, 679-689.

63. De Zotti, M.; Biondi, B.; Formaggio, F.; Toniolo, C.; Stella, L.; Park, Y.; Hahm, K. S. J Pept Sci 2009, 15, 615-619.

64. Harzer, U., Bechinger, B. Biochemistry 2000, 39, 13106-13114.

65. Knorr, R.; Trzeciak, A.; Bannwarth, W.; Gillessen, D. Tetrahedron Lett 1989, 30, 1927-1930.

66. König, W.; Geiger, R. Chem Ber 1970, 103, 788-798.

67. Stella, L.; Mazzuca, C.; Venanzi, M.; Palleschi, A.; Didoné, M.; Formaggio, F.; Toniolo, C.; Pispisa, B. Biophys J 2004, 86, 936-945.

68. Bobone, S.; Gerelli, Y.; De Zotti, M.; Bocchinfuso, G.; Farrotti, A.; Orioni, B.; Sebastiani, F.; Latter, E.; Penfold, J.; Senesi, R.; Formaggio, F.; Palleschi, A.; Toniolo, C.; Fragneto, G.; Stella, L. Biochim Biophys Acta,2013, 1828, 1013-1024.

69. Stewart, J. C. M. Anal Biochem 1980, 104, 10-14.

70. Bocchinfuso, G.; Bobone, S.; Palleschi, A.; Stella, L. Cell Mol Life Sci 2011, 68, 2281-2301.

71. Roversi, D.; Luca, V.; Aureli, S.; Park, Y.; Mangoni, M. L.; Stella L. ACS Chem Biol 2014, 9, 2003-2007.

72. Mazzuca, C.; Orioni, B.; Coletta, M.; Formaggio, F.; Toniolo, C.; Maulucci, G.; De Spirito, M.; Pispisa, B.; Venanzi M.; Stella, L. Biophys J 2010, 99, 1791-1800.

73. Bobone, S.; Bocchinfuso, G.; Park, Y.; Palleschi, A.; Hahm, K.-S.; Stella, L. J Pept Sci 2013, 19, 758-769.

74. Lehrer, S. S.; Leavis, P. C. Methods Enzymol 1978, 49, 222-236.

75. Goormaghtigh, E.; Raussens, V.; Ruysschaert, J. M. Biochim Biophys Acta 1999, 1422, 105-185.

76. Kuĉerka, N.; Tristram-Nagle, S.; Nagle, J. F. J Membr Biol 2005, 208, 193-202.

77. Nagaraj, R.; Balaram, P. Tetrahedron 1981, 37, 2001-2005.

78. Brückner, H.; Currle, M. In Second Forum on Peptides; Aubry, A., Marraud, M., Vitoux, B., Eds.; Libbey Eurotext: London, 1989; pp 251-255.

79. Wenschuh, H.; Beyermann, M.; Krause, E.; Brudel, M.; Winter, R.; Schumann, M.; Carpino, L. A.; Bienert, M. J Org Chem 1994, 59, 3275-3280.

80. Formaggio, F.; Broxterman, Q. B.; Toniolo, C. In Houben-Weyl: Methods of Organic Synthesis; Synthesis of Peptides and Peptidomimetics; Goodman, M.; Felix, A.; Moroder, L.; Toniolo, C., Eds.; Vol. E22c; Thieme: Stuttgart, Germany, 2003; pp 292-310.

81. Carpino, L. A. J Am Chem Soc 1993, 115, 4397-4398.

82. Beychok, S. In Poly-α-Amino Acids: Protein Models for Conformational Studies; Fasman, G. D., Ed.; Dekker: New York, 1967; pp 293-337.

83. Goodman, M.; Toniolo, C. Biopolymers 1968, 6, 1673-1689.

84. Manning, M. C.; Woody, R. W. Biopolymers 1992, 31, 569-586.

85. Toniolo, C.; Polese, A.; Formaggio, F.; Crisma, M.; Kamphuis, J. J Am Chem Soc 1996, 118, 2744-2745.

86. Pazos, I. M.; Roesch, R. M.; Gai, F. Chem Phys Lett 2013, 563, 93-96.

87. White, S. H.; Wimley, W. C. Biochim Biophys Acta 1998, 1376, 339-352.

88. Orioni, B.; Bocchinfuso, G.; Kim, J. Y.; Palleschi, A.; Grande, G.; Bobone, S.; Park, Y.; Kim, J. I.; Hahm, K. S.; Stella, L. Biochim Biophys Acta 2009, 1788, 1523-1533.

89. Wu, Y.; Huang, H.W.; Olah, G.A. Biophys J 1990, 57, 797-806.

90. Bechinger, B. Biochim Biophys Acta 1999, 1462, 157-183.

91. Dave, P.C.; Billington, E.; Pan, Y.; Straus, S.K. Biophys J 2005, 89, 2434-2442.

92. Ye, S.; Li, H.; Wei, F.; Jasensky, J.; Boughton, A.P.: Yang, P.; Chen, Z. J Am Chem Soc 2012, 134, 6237-6243.

93. Spaar, A.; Münster, C.; Salditt, T. Biophys J 2004, 87, 396-407.

94. Bertelsen, K.; Paaske, B.; Thøgersen, L.; Tajkhorshid, E.; Schiøtt, B.; Skrydstrup, T.; Nielsen, N. C.; Vosegaard, T. J Am Chem Soc 2009, 131, 18335-18342.

95. Dittmer, J.; Thøgersen, L.; Underhaug, J.; Bertelsen, K.; Vosegaard, T.; Pedersen, J. M.; Schiøtt, B.; Tajkhorshid, E.; Skrydstrup, T.; Nielsen, N. C. J Phys Chem B 2009, 113, 6928-6937.

Table I Acronyms and Amino Acid Sequences of the Peptides Synthesized and Studied in This Work

Acronym	Amino Acid Sequence
AlaP	Ac-Aib-Pro-Aib-Ala-Aib-Ala-Glu(OMe)-Aib-Val-Aib-Gly-Leu-Aib-Pro-Val-Aib-Aib-Glu(OMe)-Glu(OMe)-Phol
Ala4	Ac-Aib-Pro-Aib-**Phe$_{CN}$**-Aib-Ala-Glu(OMe)-Aib-Val-Aib-Gly-Leu-Aib-Pro-Val-Aib-Aib-Glu(OMe)-Glu(OMe)-Phol
Ala9	Ac-Aib-Pro-Aib-Ala-Aib-Ala-Glu(OMe)-Aib-**Phe$_{CN}$**-Aib-Gly-Leu-Aib-Pro-Val-Aib-Aib-Glu(OMe)-Glu(OMe)-Phol
Ala15	Ac-Aib-Pro-Aib-Ala-Aib-Ala-Glu(OMe)-Aib-Val-Aib-Gly-Leu-Aib-Pro-**Phe$_{CN}$**-Aib-Aib-Glu(OMe)-Glu(OMe)-Phol
TM	Ac-Lys-Lys-(Leu-Ala)$_{10}$-Lys-Lys-NH_2
TM3	Ac-Lys-Lys-**Phe$_{CN}$**-Ala-(Leu-Ala)$_9$-Lys-Lys-NH_2
TM11	Ac-Lys-Lys-(Leu-Ala)$_4$-**Phe$_{CN}$**-Ala-(Leu-Ala)$_5$-Lys-Lys-NH_2

Table II Position and Width of the IR Absorption Band of the Cyano Probe in a Membrane Environment

Peptide	Maximum (cm^{-1})	FWHM (cm^{-1})
Ala4	2229	10
Ala9	2229	10
Ala15	2229	11
TM3	2228	10
TM11	2230	6

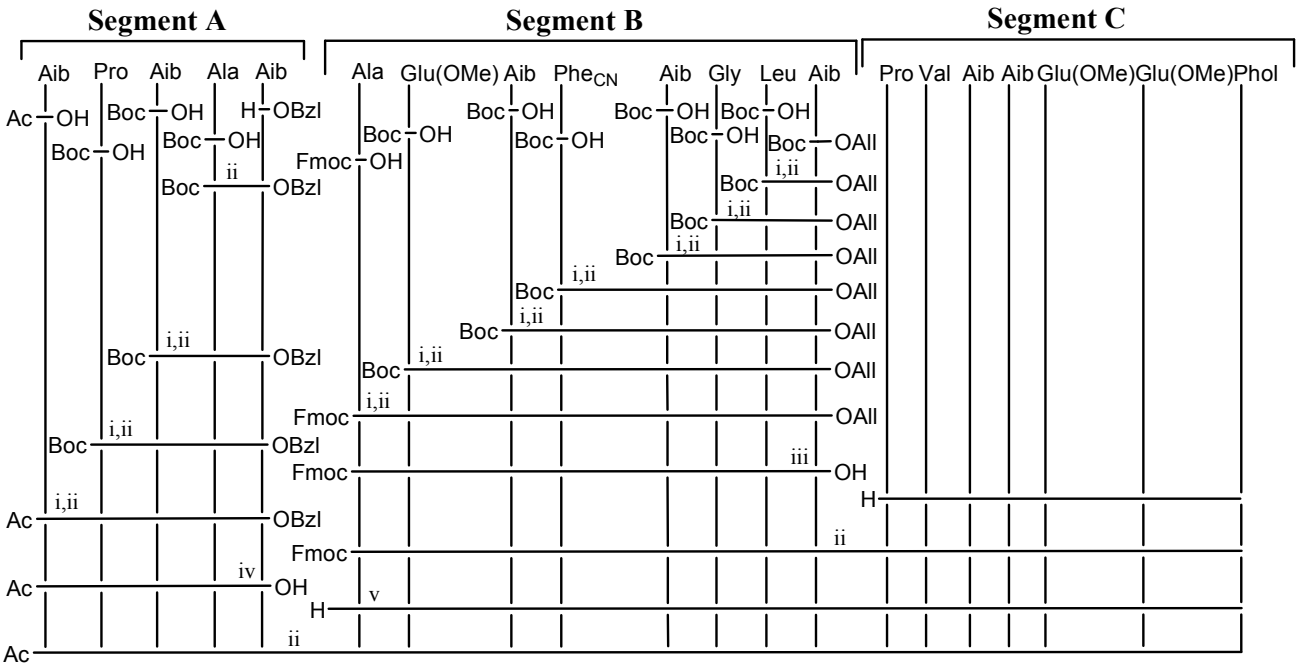

Scheme 1 Synthetic scheme used for the preparation of **Ala9**. (i) Boc removal upon treatment with TFA (10 eq.) in anhydrous DCM for 2 hr. (ii) Coupling reaction with EDC/HOAt; NMM was added to keep pH = 8. (iii) Treatment with PhHSi (2 eq.), $Pd(PPh_3)_4$ (0.2 eq.) in anhydrous DCM. (iv) OBzl removal upon treatment with H_2/Pd in MeOH. (vi) Fmoc removal upon treatment with diethylamine in DCM, followed by flash chromatography.

Ala4	**1 2 3 4 5**	**6 7 8 9 10 11 12 13**	**14 15 16 17 18 19 20**
	Ac-U P U Phe_{CN} U	**A E U V U G L U**	**P V U U E E Phol**
	Segment A	**Segment B**	**Segment C**

Ala9	**1 2 3 4 5**	**6 7 8 9 10 11 12 13**	**14 15 16 17 18 19 20**
	Ac-U P U A U	**A E U Phe_{CN} U G L U**	**P V U U E E Phol**
	Segment A	**Segment B**	**Segment C**

Ala15	**1 2 3 4 5**	**6 7 8 9 10 11 12 13**	**14 15 16 17 18 19 20**
	Ac-U P U A U	**A E U V U G L U**	**P Phe_{CN} U U E E Phol**
	Segment A	**Segment B**	**Segment C**

Scheme 2 Strategies of synthesis of the three Phe_{CN}-containing **AlaP** analogs, where **U** is Aib and **E** is Glu(OMe).

FIGURE LEGENDS

Figure 1 Fluorescence emission spectra of the **AlaP** analogs: **Ala4** (full line), **Ala9** (dashed line), **Ala15** (dotted line). Conditions: $\lambda_{exc.}$= 240 nm, room temperature, 10 mM phosphate buffer, 140 mM NaCl, 0.1 mM EDTA (pH 7.4). Peptide concentration 1 μM.

Figure 2 Far-UV CD spectra of **AlaP** and its three analogs in MeOH solution (**A**) and 100mM SDS in H_2O (**B**), and of **TM** and its two analogs in MeOH solution (**C**) and 100mM SDS in H_2O (**D**). Peptide concentration: 0.1 mM.

Figure 3 Time-resolved fluorescence decays of **Ala9** at different peptide concentrations: 0.19 μM, 1.15 μM ,and 19.2 μM. Conditions: $\lambda_{exc.}$= 240 nm; $\lambda_{em.}$= 295 nm, room temperature, 10 mM phosphate buffer, 140 mM NaCl, 0.1 mM EDTA (pH 7.4).

Figure 4 Aggregated peptide fractions as a function of peptide concentration for **AlaP** (full circles), and its analogs **Ala4** (empty circles), **Ala9** (empty squares), and **Ala15** (empty diamonds). The full line represents just a guide for the eye.

Figure 5 Fluorescence emission spectra of **Ala15** (1 μM) in the absence and presence of increasing lipid concentrations. Conditions: [POPC]= from 0.1 to 50 μM; λ_{exc} = 240 nm; liposome diameter: 100 nm; T: 25°C.

Figure 6 Membrane-bound peptide fraction as a function of [POPC] lipid concentration for **Ala4** (empty circles), **Ala9** (empty squares), and **Ala15** (empty diamonds); [peptide]= 1 μM. The full line represents a global fit to all data (see Materials and Methods).

Figure 7 Peptide-induced leaked fraction as a function of peptide concentration for **AlaP** (full circles), and its analogs **Ala4** (empty circles), **Ala9** (empty squares), and **Ala15** (empty diamonds). Conditions: $\lambda_{exc.}$ = 490 nm; $\lambda_{em.}$ = 520 nm; [POPC]: 20 μM; Liposome diameter: 200 nm.

Figure 8 Stern-Volmer plot of **TM3** (empty circles, dotted line) and **TM11** (full circles, full line) in presence of increasing amounts of KCl. F_0 and F indicate the fluorescence intensities in the absence and presence of quencher, respectively. The solid lines represent fits to the data according to the model described in Materials and Methods.

Figure 9 Polarized ATR-FTIR spectra of **TM3** in POPC membranes (P/L 5%) in the amide I region. The full and dashed lines represent the spectra collected with parallel and perpendicular polarization with respect to the plane of incidence, respectively. The ratio of the absorbance values obtained in the two spectra (dichroic ratio) indicates a transmembrane orientation (see Results and Discussion).

Figure 10 ATR-FTIR spectrum of **Ala15** in POPC lipids at P/L 15%.

Figure 11 Phe_{CN} absorption band of **TM3** (empty circles, dashed line) and **TM11** (full circles, solid line) in POPC at P/L= 5%. Circles: experimental data: lines: Gaussian fits.

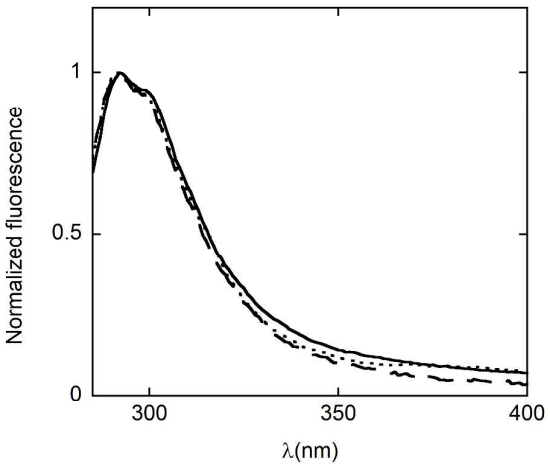

Figure 1

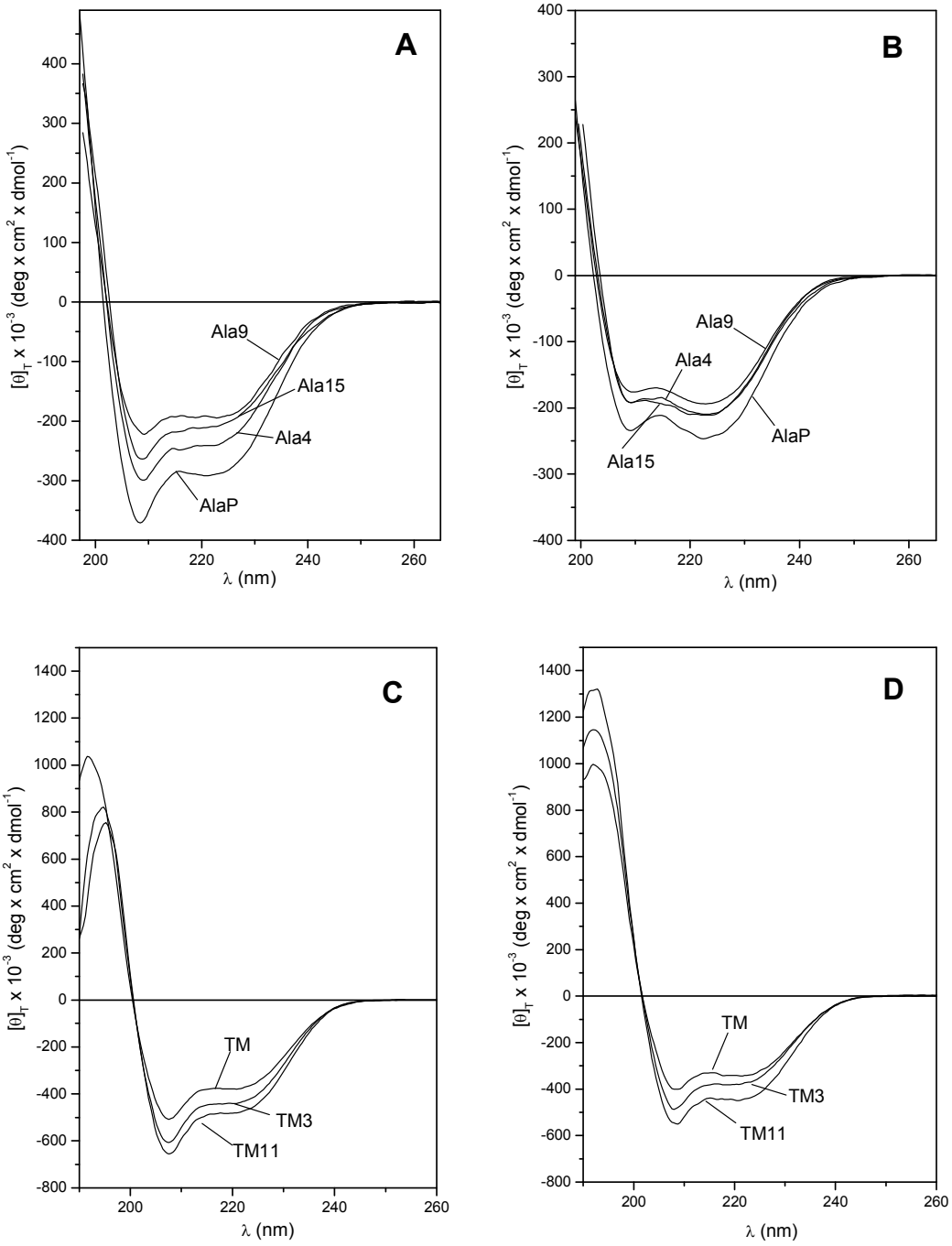
A
B
C
D
Ala9
Ala15
Ala4
AlaP
TM
TM3
TM11
λ (nm)
[θ]T x 10-3 (deg x cm2 x dmol-1)

Figure 2

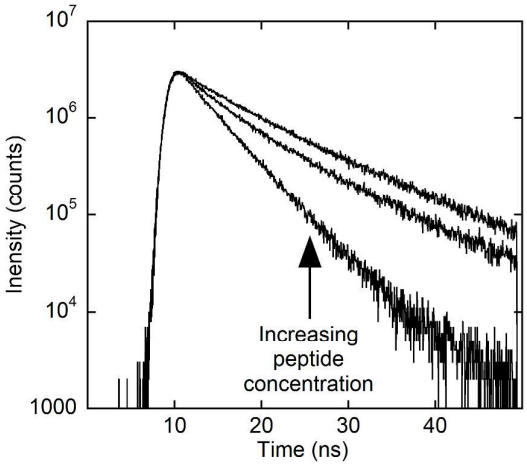
10^7
10^6
10^5
10^4
1000
Inensity (counts)
10
20
30
40
Time (ns)
Increasing
peptide
concentration

Figure 3

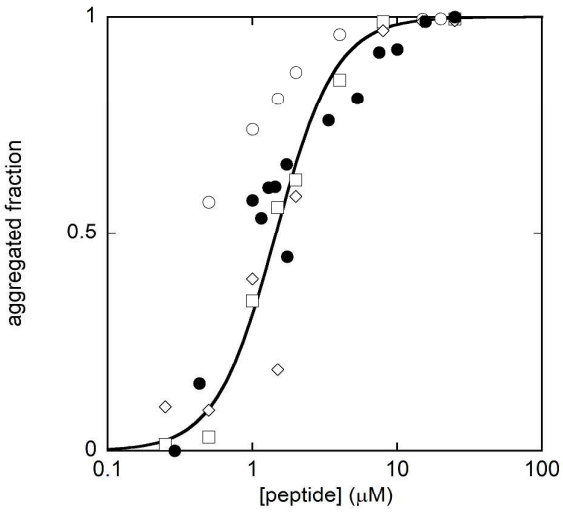

Figure 4

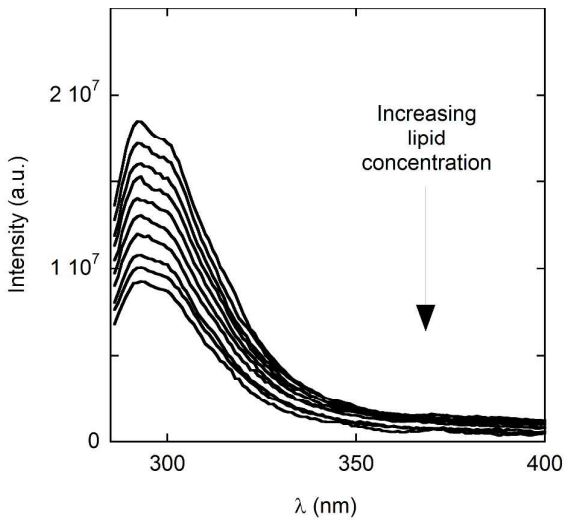
2 10^7
1 10^7
0
Intensity (a.u.)
300
350
400
λ (nm)
Increasing
lipid
concentration

Figure 5

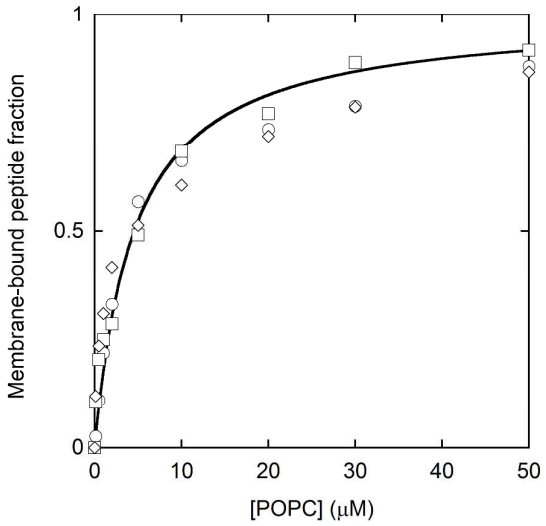

Figure 6

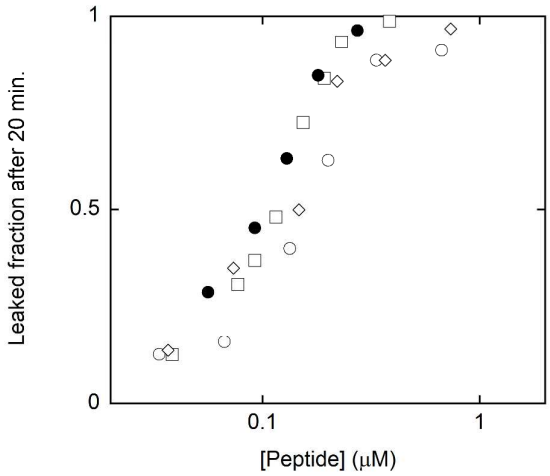

Figure 7

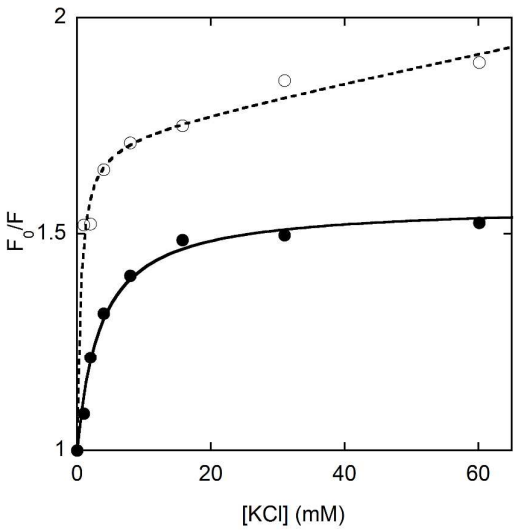

Figure 8

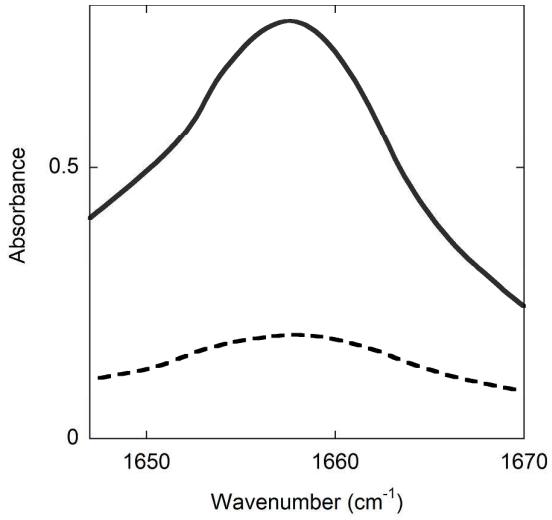

Figure 9

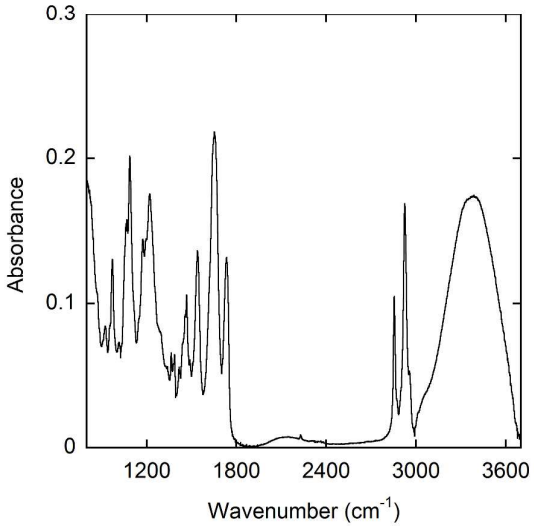
0.3
0.2
0.1
0
Absorbance
1200
1800
2400
3000
3600
Wavenumber (cm-1)

Figure 10

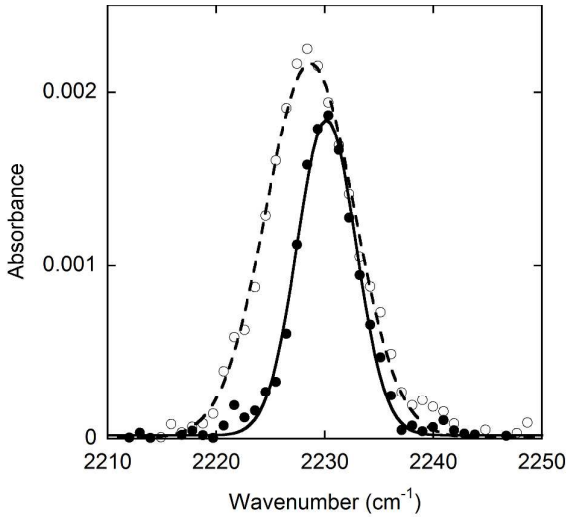
0.002
0.001
0
Absorbance
2210
2220
2230
2240
2250
Wavenumber (cm-1)

Figure 11